Journal of
Marine Science and Engineering

MDPI

Article

Development of a Position Measuring Device of a Deep-Sea Pipeline Based on Flange Center Positioning

Zhuo Wang [1,*], Hong-xing Dang [1], Tao Wang [2] and Bo Zhang [1]

[1] College of Mechanical and Electrical Engineering, Harbin Engineering University, Harbin 150001, China; danghongxing@hrbeu.edu.cn (H.-x.D.); zhangbo_heu@hrbeu.edu.cn (B.Z.)
[2] School of Mechanical Engineering, Hebei University of Technology, Tianjin 300401, China; 18846166436@hrbeu.edu.cn
* Correspondence: wangzhuo_heu@hrbeu.edu.cn

Received: 15 December 2019; Accepted: 27 January 2020; Published: 1 February 2020

Abstract: A deep-sea pipeline position and attitude-measuring device based on pipeline outer circle positioning can measure the spatial relative positions of the end faces of two oil pipelines in the deep sea. This device can provide the necessary data to make a transition pipeline connecting two sections of oil pipelines together. However, after analyzing the data measured by this device, it is found that the measurement data has a large error because the error transmission coefficient of the measurement value is too large. In order to reduce the error transfer coefficient, a new measuring device for measuring the posture of deep-sea pipelines by a tensioning rope was proposed. Unlike previous measuring devices, this measuring device is based on the positioning of the flange center of the pipe instead of the pin on the outer circle of the pipe. With the comparison of positioning methods between fixing in the center of flange and fixing the outer wall of pipeline, the former can reduce the transition matrix in the process of solving the relative position of the two pipes, and then reduce the magnification of the measurement sensor error. It also reduces two measurement parameters. The solving formula of the position and attitude of the measuring device based on the outer circle positioning of the pipeline is analyzed. It is proved that the error transmission coefficient of the measuring device based on the flange center positioning is smaller. Experiments show that compared with the positioning method based on the outer circle of the pipe, the positioning method based on the flange center has a higher accuracy.

Keywords: oil pipeline; transition matrix; error transfer coefficient; based on flange center

1. Introduction

The ocean is rich in oil resources below 500 meters, and the transportation of oil from the deep sea to the land requires the use of oil pipelines in the deep sea [1,2]. In order to incorporate the pipeline of the new oilfield into the already laid submarine pipeline network, it is necessary to connect the two fixed-point pipelines together on the seabed [3,4]. At present, the main method of connecting deep-sea pipeline is to connect the two ends of the prepared transition pipeline to the oil outlet of the old pipeline and the oil inlet of the new pipeline [5]. The transition ducts that perfectly match the two sections of the pipeline need to accurately measure the relative position of the new and old pipelines. Therefore, deep-sea exploration equipment and technology have become hotspots in the international marine engineering community [6,7].

The location measurement of submarine pipelines mainly includes the following methods: underwater acoustic measurement, satellite positioning, and rope measurement [8]. Acoustic measurement is used by most underwater measurement operations. However, the underwater

acoustic measurement system requires a large amount of equipment, and the installation work takes a long time. It is generally used for large-area mapping and geological exploration of seabed topography, and is rarely used in the measurement of underwater pipeline poses [9,10]. Satellite positioning technology is applied to a variety of underwater positioning tasks. For example, a measurement system consisting of underwater GPS and a single beam measuring instrument can effectively solve underwater high-precision positioning problems [11,12]. Drawstring measurements include traditional tensioning rope measurements and intelligent drawstring measurements. A diver carrying a measuring tool under water carries out the traditional tensioning rope measurement method [13]. The drawstring intelligent measurement method is suitable for a deep water environment, and it has the characteristics of high measurement accuracy and real-time dynamic measurement [14]. For example, the unmanned drawstring system developed by NGI of Norway, which is not limited by water depth, has a length accuracy of ±10 cm and an angular accuracy of ±0.5° [15]. Professor Wang Liquan of Harbin Engineering University in China proposed a deep-sea measurement system on the pipeline attitude. Its maximum working water depth is 1500 m, which can achieve a measurement accuracy of ±50 mm and ±1° within a 5 m working range [16]. In addition to the above methods, multi-beam sounding technology, inertial navigation measurement system, and side scan sonar are more and more used in the positioning and detection of underwater pipelines [17,18].

The article mainly studies the intelligent measurement method of the drawstring. By analyzing the error of the measuring device based on the outer circle positioning of the pipeline, it is determined that the existing measuring device can be optimized to improve the accuracy. Based on this, a cable-measuring device based on the center point of the flange was designed, its mathematical model was solved, and the error transfer coefficient was analyzed.

2. Measurement System and Experimental Method Based on Pipeline Circular Positioning

2.1. Composition of the Measurement System

On the working boat, the staff on board sends one instruction to the lower position machine of the ROV (Remote Operated Vehicle) through the umbilical cable, so that the ROV helps the measuring device to obtain the variable parameters for calculating the relative position of the two pipeline spaces, and then transmits the measurement data to the upper computer for calculation. The measuring system measures the rocking angle of the measuring device I and the measuring device II with respect to the absolute vertical plane and the tilting pitch angle with the absolute horizontal plane by means of an orthogonal inclination sensor on the measuring device. There are two magnetically coupled encoders on each measuring device for obtaining the horizontal and vertical corners of the projecting arm of the measuring device. In addition to this, the measuring device II has one more rope length-detecting device than the measuring device I connected to the magnetron cable winch for detecting the distance between the two measuring devices.

The deep-sea pipeline position and attitude measuring device based on the outer circle positioning of the pipeline mainly includes the measuring device I, the measuring device II, the base I, the base II, the drawstring, and the drawstring winch, as shown in Figure 1.

The orthogonal inclination sensor and the encoder mounted on the measuring device are connected to the positioning base. The positioning base I and the base II have the same structure, and they are positioning platforms for connecting the measuring device to the pipe.

Figure 1. Measuring device based on the outer circle positioning of the pipeline.

2.2. Method for Measuring the Relative Position of Two Pipes

2.2.1. Mathematical Model and Solution Formula of the Measuring Device Based on the Outer Circle Positioning of the Pipeline

Figure 2 is the mathematical model I of the deep-sea pipeline position and orientation-measuring device based on pipeline outer circle positioning. P_r and P_b are the center points of the end faces of pipe I and pipe II, respectively. The pull-out points A and B of the tensioning rope are parallel planes of the two flange end faces, which are used as reference planes of the respective measuring devices, and the centerlines of the pipes are intersected at O_r and O_4, respectively. With O_r and O_4 as the origin, absolute coordinate systems Ω_R and Ω_4 are established, respectively, and the z-axis of these two coordinate systems are in the same direction. Set the reference coordinate system Ω_1 with O_r as the origin of the pipe centerline as the y-axis. The reference coordinate system Ω_2 is obtained by positively translating Ω_1 along its z-axis by R_1. Rotate Ω_2 around the z-axis until the x-axis coincides with the projection in plane A to establish the reference coordinate system Ω_3. Create the reference coordinate system Ω_5 with reference to Ω_1.

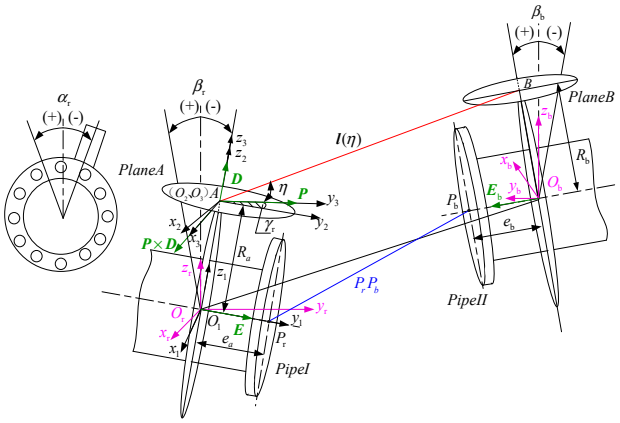

Figure 2. Mathematical model I of the measuring device based on the outer circle positioning of the pipeline.

Reference [16] solves the mathematical model I. Equation (1) is the calculation formula for the distance parameter and angle parameter between two pipes. In this way, the host computer can use

this algorithm and the data measured by the sensor to calculate the relative distance between the centers and the relative angle of the two pipe end faces.

$$\begin{aligned}
P_rP_{bx} =& -e_bS\Delta pC\beta_b + R_aS\alpha_r + LS\eta S\alpha_r + R_bC\Delta pS\alpha_b - LC\eta S\gamma_rC\alpha_r - R_bS\Delta pC\alpha_bS\beta_b \\
P_rP_{by} =& -R_aC\alpha_rS\beta_r + LC\eta C\gamma_rC\beta_r - LC\eta S\gamma_rS\alpha_rS\beta_r - e_bC\Delta pC\beta_b - R_bS\Delta pS\alpha_b - e_rC\beta_b - LS\eta C\alpha_rS\beta_r - R_bC\Delta pC\alpha_bS\beta_b \\
P_rP_{bz} =& -e_rS\beta_r + e_bS\beta_b - R_bC\alpha_bC\beta_b + R_aC\alpha_rC\beta_r + LC\eta S\beta_rC\gamma_r + LC\eta S\gamma_rS\alpha_rC\beta_r + LS\eta C\alpha_rC\beta_r \\
\xi x =& 90^\circ - \xi y = 90^\circ - \Delta p \\
\xi z =& \beta_b - \beta_r
\end{aligned} \tag{1}$$

where P_RP_{bx}, P_RP_{by}, and P_RP_{bz} are the projection values of the vectors of the two pipeline centers in the X-axis, Y-axis, and Z-axis directions of the absolute coordinate system Ω_R. ξx_1, ξy_1, and ξz_1 are the angles formed by the axis of pipe II and the X, Y, and Z axes of the absolute coordinate system Ω_R. α_r and α_b are the angles between the x-axis of the orthogonal tilt sensor of measurement device I and measurement device II and the absolute horizontal plane. β_r and β_b are the measurement device I and the measurement device, respectively. The angle is between the Y-axis of the orthogonal tilt sensor of the II and the absolute horizontal plane. γ_r and γ_b are the horizontal swing angles of the measuring rope in the reference coordinate system Ω_1 and the reference coordinate system Ω_2, respectively. R_a and R_b are the distance from the extension point of the tensioning rope to the mounting base I and the mounting base II, respectively. e_a and e_b are the distance between the mounting base I and the end face of pipe I and pipe II, respectively. L is the distance between the pullout points A and B. According to reference 16, L can be obtained by Equation (2).

$$\begin{aligned}
L^2 &= c^2 + l^2 \\
l &= \frac{6S_r}{6+T^2\theta_r+T\theta_rT\theta_b+T^2\theta_b} \\
c &= \frac{3S_r(T\theta_r+T\theta_b)}{6+T^2\theta_r+T\theta_rT\theta_b+T^2\theta_b}
\end{aligned} \tag{2}$$

where: S = sin (); C = cos (); T = tan (). l is the actual length of the tensioning rope. c is the relative height of the two measuring devices. S_r is the measuring length of the tensioning rope. θ_r and θ_b are the pitching angles of the tensioning rope in the reference coordinate system Ω_1 and the reference coordinate system Ω_2, respectively.

2.2.2. Measurement Test

The measurement experiment is mainly performed to compare the experimental data obtained by the measuring device with the actual relative position of the space of the two pipes in the case of simulating two pipes in different postures. The measurement experiment should be divided into the following steps.

(1) In the pipeline pose measurement experiment based on the outer circle positioning of the pipeline, it is first necessary to initialize the measuring device. That is, the position of pipe II is adjusted to ensure that the end faces of the two pipe flanges are parallel, and the pipe axes are coincident, as shown in Figure 3. Record the initial values of each sensor at this time. In addition to this, it is also necessary to measure the length of the two take-off points of the drawstring on the measuring device I and the measuring device II to the two pipe axes and to the horizontal distance to the end faces of the two pipes.

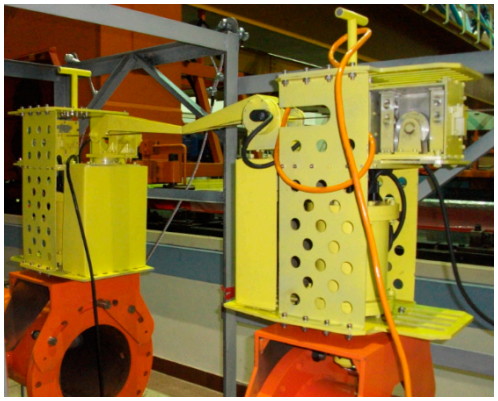

Figure 3. Initialization of the measuring device.

(2) After initialization, we will move pipe II to the next position and adjust the pitch angle and swing angle of pipe I, and then manipulate the magnetic power winch to tension the rope. At this time, the lower computer will obtain the data of each sensor and transmit it to the upper computer through the signal line. Next, the distance and angle of the flange center of pipe I and pipe II are measured by a laser range finder and an angle measuring instrument as reference values, and pipe II is moved to the next position to measure a plurality of sets of data.

(3) The measurement experiment based on the positioning of the outer circle of the pipeline uses a laser rangefinder to adjust the distance between the two pipeline centers to 2 m, 3 m, 4 m, 5 m, 6 m, and 7 m, and the angle measuring instrument is used to adjust the angles parameters ξx_1, ξy_1, and ξz_1 formed by the axis of pipe II and the X, Y, and Z axes of the absolute coordinate system Ω_R. It corresponds to the actual value in Table 1. Then the host computer calculates the angle parameters ξx_1, ξy_1, and ξz_1 and the length parameters $P_R P_{bx}$, $P_R P_{by}$, and $P_R P_{bz}$, which are the projection values of the vectors of the two pipeline centers in the X-axis, Y-axis, and Z-axis directions of the absolute coordinate system Ω_R. It corresponds to the measurements in Table 1.

Table 1. Experimental data of a measuring device based on the outer circle positioning of the pipe.

Component of Measurements	Classification	2 m	3 m	4 m	5 m	6 m	7 m
$P_r P_{bx}$	actual value (mm)	0.0	0.0	0.0	0.0	0.0	0.0
	measurements (mm)	5.4	11.2	25.4	21.3	38.3	40.4
$P_r P_{by}$	actual value (mm)	2000.0	3000.0	4000.0	5000.0	6000.0	7000.0
	measurements (mm)	1981.5	3009.9	4012.4	5022.5	6025.7	7032.6
$P_r P_{bz}$	actual value (mm)	0.0	0.0	0.0	0.0	0.0	0.0
	measurements (mm)	−6.6	12.2	12.8	27.7	54.5	68.8
ξx_1	actual value (mm)	0.0	0.0	0.0	0.0	0.0	0.0
	measurements (mm)	0.2	0.5	0.8	1.1	1.2	1.1
ξy_1	actual value (mm)	90.0	90.0	90.0	90.0	90.0	90.0
	measurements (mm)	89.8	89.5	89.2	88.9	88.8	88.9
ξz_1	actual value (mm)	0.0	0.0	0.0	0.0	0.0	0.0
	measurements (mm)	0.3	0.2	0.8	0.5	0.7	1.2

2.3. Error Analysis

Since the measurements used to solve the mathematical model I are directly measured, the deterministic error propagation rate of the measurement system based on the outer circle positioning of the pipeline is

$$E(y) = \frac{\partial f}{\partial x_1} E(x_1) + \frac{\partial f}{\partial x_2} E(x_2) + \cdots + \frac{\partial f}{\partial x_i} E(x_i), \tag{3}$$

where: $E(x_i)$ is the deterministic error of each measurement and $\partial f / \partial x_i$ is the error transfer coefficient of the corresponding measurement; $E(y)$ is the sum of the errors of each measurement. The error value of the orthogonal inclination sensor is ±0.1°. The value of the error transfer coefficient of some measurements calculated by Equation (3) is large, which causes the error of the sensor to be amplified. This may be because the number of transition matrices based on the mathematical model I is large, resulting in an increase in the magnification of the error transfer coefficient. Therefore, optimizing the structure of the measuring device can reduce the number of transition matrices in the solution process and improve the measurement accuracy.

3. Design of the Measuring Device Based on Flange Center Positioning

3.1. Overall Design

If the take-off point of the drawstring between the two measuring devices is on the axis of the pipe, the number of transition matrices can be reduced, and since the two measurement parameters R_a and R_b are no longer needed, the errors caused to the measurement system are eliminated. The measuring device is positioned using the outer end face of the flange so that the take-up point of the drawstring is on the axis of the pipe. Considering that the flange is more resistant to corrosion than the pipe, it can avoid installation errors introduced by pipe corrosion [19]. Therefore, a pipe position measuring device based on flange positioning is proposed, and its schematic diagram is shown in Figure 4.

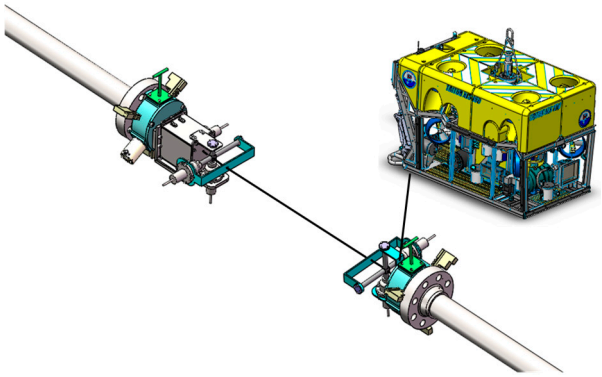

Figure 4. Schematic diagram of the measurement system based on flange center positioning.

The measuring device based on flange center positioning secures flange and electric drive three-jaw chuck, and it is positioned and mounted by the three-jaw chuck. This type of structure can better meet the alignment accuracy requirements of the measuring device.

The orthogonal tilt sensor was fixed in the three-jaw chuck. The angle measuring mechanism was fixed on the other side of the flange, consisting of a horizontal axis and a vertical axis that were centered and intersected at one point, which was also the take-up point of the drawstring on the axis of the pipe. The measuring device II has one more rope length detecting device located between the angle measuring mechanism and the flange.

3.2. Building and Solving the Mathematical Model of the Deep-Sea Pipeline Pose Measurement Device Based on Flange Positioning

The mathematical model II for establishing the deep-sea pipeline pose measurement device based on flange positioning is shown in Figure 5. Then, we analyzed this mathematical model II in order to solve the angles parameters ξx_2, ξy_2, and ξz_2 formed by the axis of pipe II and the X, Y, and Z axes of the absolute coordinate system Ω_R and the length parameters $O_R O_{bx}$, $O_R O_{by}$, and $O_R O_{bz}$, which are the projection values of the vectors of the two pipeline centers in the X-axis, Y-axis, and Z-axis directions of the absolute coordinate system Ω_R. All subsequent formulas are based on this mathematical model II.

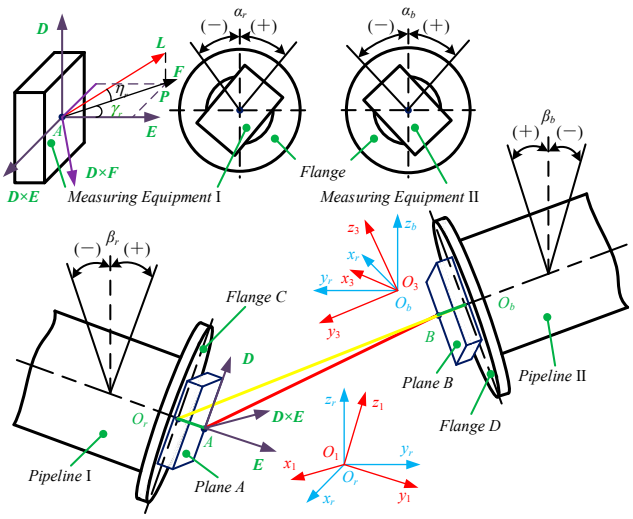

Figure 5. Mathematical model II of the measuring device based on flange center positioning.

In the mathematical model II, O_r and O_b are the center points of the end faces of pipe I and pipe II, respectively. The two flange end faces correspond to the plane C and the plane D, respectively, and the lead point A and the lead point B of the over-pull line are respectively made to plane A and plane B parallel to the flange end faces. The central axis of pipe I and the planes A and C intersect the points A and O_r, respectively, and the central axis of the pipe of pipe II and the planes B and D intersect at points B and O_b, respectively. We can establish the absolute coordinate system Ω_R with O_r as the origin. The coordinate system Ω_R is rotated about the x-axis and the y-axis to β_r and α_r to establish the reference coordinate system Ω_1. β_r and α_r are the rocking angle of the measuring device I with respect to the pipe axis and the pitch angle of the absolute horizontal plane e, respectively. The absolute coordinate system Ω_b and the reference coordinate system Ω_3 are established. γ_r and θ_r are the horizontal swing angle and the pitch angle of the tensioning rope in the reference coordinate system Ω_1, respectively. Similarly, α_b, β_b, γ_b, and θ_b can be expressed, and S_r is the measuring length of the tensioning rope.

For the measuring device I, there are rotation operators $Rot_x(\beta_r)$ and $Rot_y(\alpha_r)$ between the coordinate systems Ω_1 and Ω_R, as shown in Equation (4). In the following Equations, S = sin (); C = cos (); T = tan ().

$$\begin{aligned} Rot_x(\beta_r) &= \begin{bmatrix} 1 & 0 & 0 & 0 \\ 0 & C\beta_r & -S\beta_r & 0 \\ 0 & S\beta_r & C\beta_r & 0 \\ 0 & 0 & 0 & 1 \end{bmatrix} \\ Rot_y(\alpha_r) &= \begin{bmatrix} C\alpha_r & 0 & S\alpha_r & 0 \\ 0 & 1 & 0 & 0 \\ -S\alpha_r & 0 & C\alpha_r & 0 \\ 0 & 0 & 0 & 1 \end{bmatrix} \end{aligned} \tag{4}$$

Therefore, the homogeneous transformation matrix ${}^{R}_{1}T$ between the coordinate systems Ω_1 and Ω_R is calculated by the Equation (5).

$${}^{R}_{1}T = Rot_x(\beta_r) \cdot Rot_y(\alpha_r). \tag{5}$$

The unit vectors $\vec{E} = \begin{bmatrix} 0 & 1 & 0 \end{bmatrix}^T$ and $\vec{D} = \begin{bmatrix} 0 & 0 & 1 \end{bmatrix}^T$ are introduced in the coordinate system Ω_1, and the coordinates of $\vec{E_R}$ and $\vec{D_R}$ are the unit vectors $\vec{E}$ and $\vec{D}$ in the absolute coordinate system Ω_R, respectively. They are calculated by the Equation (6).

$$\begin{cases} \vec{E_R} = Rot_x(\beta_r)\vec{E} = \begin{bmatrix} 0 & C\beta_r & S\beta_r \end{bmatrix}^T \\ \vec{D_R} = {}^R_1T\vec{D} = \begin{bmatrix} S\alpha_r & -S\beta_r C\alpha_r & C\alpha_r C\beta_r \end{bmatrix}^T \end{cases}. \tag{6}$$

The coordinate system Ω_1 is determined to be ($\vec{E} \times \vec{D}$,$\vec{E}$,$\vec{D}$) according to the unit vectors $\vec{E}$ and $\vec{D}$. Equation (7) is the coordinate of $\vec{E} \times \vec{D}$ in the coordinate system Ω_1.

$$\vec{E} \times \vec{D} = \begin{bmatrix} C\alpha_r & S\alpha_r S\beta_r & -C\beta_r S\alpha_r \end{bmatrix}^T. \tag{7}$$

$\vec{L}$ is the unit vector of $\vec{AB}$ and $\vec{L}$ is projected as $\vec{AP}$ in the coordinate system Ω_1 horizontal plane. Taking the vector $\vec{F}$ along the $\vec{AP}$ direction establishes the coordinate system Ω_2($\vec{F} \times \vec{D}$,$\vec{F}$,$\vec{D}$). In Ω_2, the coordinate of $\vec{F}$ is $\begin{bmatrix} 0 & 1 & 0 \end{bmatrix}^T$. There is a rotation operator $Rot_z(\gamma_r)$ between the coordinate system Ω_2 and Ω_1, and the corresponding homogeneous transformation matrix ${}^1_2T$ is Equation (8).

$${}^1_2T = Rot_z(\gamma_r) = \begin{bmatrix} C\gamma_r & -S\gamma_r & 0 & 0 \\ S\gamma_r & C\gamma_r & 0 & 0 \\ 0 & 0 & 1 & 0 \\ 0 & 0 & 0 & 1 \end{bmatrix}. \tag{8}$$

Therefore, the transformation matrix ${}^R_2T$ between coordinate system Ω_2 and coordinate system Ω_R can be calculated by the Equation (9).

$${}^R_2T = {}^R_1T \cdot {}^1_2T = \begin{bmatrix} C\alpha_r C\gamma_r & -S\gamma_r C\alpha_r & S\alpha_r & 0 \\ C\beta_r S\gamma_r + S\alpha_r S\beta_r C\gamma_r & C\gamma_r C\beta_r - S\alpha_r S\beta_r S\gamma_r & -C\alpha_r S\beta_r & 0 \\ S\beta_r S\gamma_r - C\beta_r S\alpha_r C\gamma_r & S\beta_r C\gamma_r + C\beta_r S\alpha_r S\gamma_r & C\alpha_r C\beta_r & 0 \\ 0 & 0 & 0 & 1 \end{bmatrix}. \tag{9}$$

F_R is the coordinates of $\vec{F}$ in the absolute coordinate system Ω_R. F_R can be calculated by Equation (10).

$$F_R = \begin{bmatrix} -S\gamma_r C\alpha_r \\ -S\alpha_r S\beta_r S\gamma_r + C\gamma_r C\beta_r \\ S\alpha_r C\beta_r S\gamma_r + C\gamma_r S\beta_r \end{bmatrix}^T. \tag{10}$$

Let η be the angle between $\vec{AB}$ and plane A. Then the coordinate $\vec{L_R}$, which is the unit vector $\vec{L}$ in the absolute coordinate system Ω_R, can be calculated by Equation (11):

$$\vec{L_R} = C\eta \cdot \vec{F_R} + S\eta \cdot \vec{D_R}. \tag{11}$$

Let a be the projection length of the distance L between the pull-out points A and B in the Z-axis direction of the absolute coordinate system Ω_R, which is $a = c/L$. The values of c and L can be solved by Equation (2). Substituting a for the Equation (11) to solve η obtains Equation (12).

$$\eta = arccos\left(\frac{aF_R \pm \sqrt{F_R^2 a^2 - (F_R^2 + D_R^2)(a^2 - D_R^2)}}{F_R^2 + D_R^2} \right). \tag{12}$$

$\vec{AB}_R$ is the coordinate of the vector $\vec{AB}$ in the coordinate system Ω_R. $\vec{AB}_b$ is the coordinate of the vector $\vec{AB}$ in the coordinate system Ω_b. $\vec{AB}_R$ can be calculated by Equation (13) according to the mathematical model II.

$$\vec{AB}_R = L\left(C\eta \cdot \vec{F}_R + S\eta \cdot \vec{D}_R\right). \tag{13}$$

Substituting η into Equation (14) can calculate $\vec{AB}_R$. Similarly, $\vec{AB}_b$ can be calculated by Equation (15).

$$\vec{AB}_R = \begin{bmatrix} L(S\eta S\alpha_r - C\eta C\alpha_r S\gamma_r) \\ LC\eta(C\beta_r C\gamma_r - S\alpha_r S\beta_r S\gamma_r) - LS\eta C\alpha_r S\beta_r \\ LC\eta(S\beta_r C\gamma_r + C\beta_r S\alpha_r S\gamma_r) + LS\eta C\alpha_r C\beta_r \end{bmatrix}, \tag{14}$$

$$\vec{AB}_b = \begin{bmatrix} L(C\eta_b C\alpha_b S\gamma_b - S\eta_b S\alpha_b) \\ LC\eta_b(S\alpha_b S\beta_b S\gamma_b - C\beta_b C\gamma_b) + LS\eta_b C\alpha_b S\beta_b \\ -LC\eta_b(S\beta_b C\gamma_b + C\beta_b S\alpha_b S\gamma_b) - LS\eta_b C\alpha_b C\beta_b \end{bmatrix}. \tag{15}$$

The coordinates of $\vec{AB}_R$ and $\vec{AB}_b$ are the two bases in space. Introducing the transition matrix P and the transition angle Δp. The transition matrix P is calculated by Equation (16). The transition angle Δp is solved by the Equation (14) to the Equation (16), and Equation (17) is result of the transition angle Δp.

$$P = \begin{bmatrix} -C\Delta p & S\Delta p & 0 \\ -S\Delta p & -C\Delta p & 0 \\ 0 & 0 & 1 \end{bmatrix}, \tag{16}$$

$$\begin{cases} C\Delta p = \frac{-AB_{Rx} \cdot AB_{bx} - AB_{Ry} \cdot AB_{by}}{AB_{bx}^2 + AB_{by}^2} \\ S\Delta p = \frac{AB_{Ry} \cdot AB_{bx} - AB_{Rx} \cdot AB_{by}}{AB_{bx}^2 + AB_{by}^2} \end{cases}. \tag{17}$$

The transition matrix P^T that makes the coordinate system Ω_b to Ω_R can be solved by the Equation (16) and the Equation (17). Since $\vec{O_rA}$ and $\vec{BO_b}$ are equal to the vertical distance from the projecting point of the tensioning rope to the end face of the flange in the two measuring devices, $\vec{O_rA}$ and $\vec{BO_b}$ can be calculated by Equation (18) according to the design size of measuring device.

$$\begin{cases} \vec{O_RA} = m_1\vec{E_r} \\ \vec{BO_b} = -m_2P^T\vec{E_b} \end{cases}, \tag{18}$$

where: m_1 and m_2 correspond to the vertical distances from the point A and the point B of the measuring device I and the measuring device II to the end faces of the flange, respectively.

From the Equation (7) and the Equation (10), the length parameters O_RO_{bx}, O_RO_{by}, and O_RO_{bz}, which are the projection values of the vectors of the two pipeline centers in the X-axis, Y-axis, and Z-axis directions of the absolute coordinate system Ω_R, can be calculated by Equation (19).

$$\begin{cases} O_RO_{bx} = \left|L(S\eta S\alpha_r - C\eta C\alpha_r S\gamma_r) - m_2S\Delta PC\beta_b\right| \\ O_RO_{by} = \left|m_1C\beta_r + LC\eta(C\beta_r C\gamma_r - S\alpha_r S\beta_r S\gamma_r) - LS\eta C\alpha_r S\beta_r + m_2C\Delta PC\beta_b\right| \\ O_RO_{bz} = \left|m_1S\beta_r + LC\eta(S\beta_r C\gamma_r + C\beta_r S\alpha_r S\gamma_r) + LS\eta C\alpha_r C\beta_r - m_2S\beta_b\right| \end{cases}. \tag{19}$$

Establish a reference coordinate system Ω_r as shown in Figure 6, and there is a rotation operator $Rot_x(\beta_r)$ between the coordinate system Ω_R and Ω_r. In Figure 6, F_1 and F_2 correspond to O_1 and O_2 in mathematical model II, respectively. Let the unit vector of the central axis of pipe I be $\vec{V_r}$, and $\begin{bmatrix} 0 & C\beta_r & S\beta_r \end{bmatrix}^T$ is the coordinate of $\vec{V_r}$ in the coordinate system Ω_R. Let the unit vector of the central axis of pipe II be $\vec{V_b}$, and $\begin{bmatrix} 0 & C\beta_b & S\beta_b \end{bmatrix}^T$ is the coordinate of $\vec{V_b}$ in the coordinate system Ω_b. $\vec{V_{bR}}$ is

the coordinate of the $\vec{V_b}$ in the coordinate system Ω_R, which is solved by Equation (20). Let $\vec{V_{ba}} = -\vec{V_{bR}}$. $\vec{V_{rr}}$, which is the coordinate of $\vec{V_r}$ in the coordinate system Ω_r, is solved by Equation (21).

$$\vec{V_{bR}} = \begin{bmatrix} -S\Delta pC\beta_b & -C\Delta pC\beta_b & S\beta_b \end{bmatrix}^T, \tag{20}$$

$$\vec{V_{rr}} = Rot_x(\beta_r)^{-1}\vec{V_r} = \begin{bmatrix} 0 & 1 & 0 \end{bmatrix}^T. \tag{21}$$

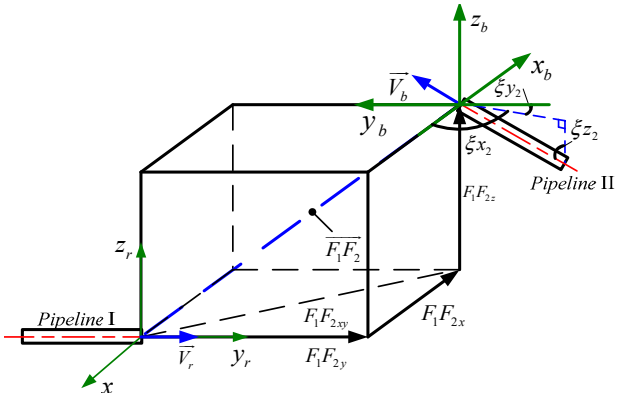

Figure 6. Schematic diagram of angle parameters.

Similarly, $\vec{V_{br}}$ which is the coordinate of $\vec{V_{ba}}$ in the coordinate system Ω_r is solved by Equation (22).

$$\vec{V_{ba}} = Rot_x(\beta_r)^{-1}\vec{V_{ba}} = \begin{bmatrix} S\Delta pC\beta_b \\ C\Delta pC\beta_rC\beta_b - S\beta_rS\beta_b \\ -C\Delta pS\beta_rC\beta_b - C\beta_rS\beta_b \end{bmatrix}^T. \tag{22}$$

The angle parameters ξx_2, ξy_2, and ξz_2 can be calculated according to the Equation (19) and the Equation (20), as shown in Equation (23).

$$\begin{cases} \xi x = 90^\circ - \xi y \\ \xi y = arctan(S\Delta pC\beta_b/(C\Delta pC\beta_rC\beta_b - S\beta_rS\beta_b)) \\ \xi z = arcsin(-C\Delta pS\beta_rC\beta_b - C\beta_rS\beta_b) \end{cases}. \tag{23}$$

3.3. Analysis of Error Transfer Coefficient

Since the mathematical model II based on the flange center positioning compared to the measuring device based on the outer circle positioning of the pipe removes the parameters R_a and R_b, the error transfer coefficient analysis is performed based on the mathematical model I of the measuring system based on the outer circle positioning of the pipe. From Equation (24), Equation (25), and Equation (26), the error transfer coefficients C_i, N_i, M_i of the length parameters O_1O_{2x}, O_1O_{2y}, $O1O_{2z}$ related to the parameters R_a and R_b can be calculated.

$$\begin{cases} C_1 = R_aC\alpha_r + LS\eta C\alpha_r + LC\eta S\alpha_rS\gamma_r \\ N_1 = R_aS\alpha_rS\beta_r + LS\eta S\alpha_rS\beta_r + LC\eta C\alpha_rS\beta_rS\gamma_r \\ N_3 = (e_rS\beta_r - R_aC\alpha_rC\beta_r - LC\alpha_rC\beta_rS\eta - LC\eta S\beta_rC\gamma_r - LC\eta C\beta_rS\alpha_rS\gamma_r) \\ M_1 = LC\eta C\alpha_rC\beta_rS\gamma_r - LC\beta_rS\eta S\alpha_r - R_aC\beta_rS\alpha_r \\ M_3 = (C\eta C\beta_rC\gamma_r - R_aC\alpha_rS\beta_r - e_rC\beta_r - LC\alpha_rS\eta S\beta_r - LC\eta S\alpha_rS\beta_rS\gamma_r) \end{cases}. \tag{24}$$

As shown in Equation (24), the coefficients C_1, N_1, M_1, N_3, and M_3 are affected by the parameters R_a, e_a, and L. Ignoring the effect of e_a on N_3, the coefficient C_1 is taken as an example to show the

variation of the relative parameters R_a and L of ${C_1}^2$ as shown in Figure 7. Figure 7 (a) corresponds to the same positive and negative α_r and γ_r, and Figure 7 (b) corresponds to the difference between α_r and γ_r. It can be seen from the figure that C_1 is mainly affected by the parameter L and it is proportional to L. The parameter R_a has little effect on ${C_1}^2$. The relative curves of the relative parameters R_a and L of ${N_1}^2$, ${M_1}^2$, ${N_3}^2$, and ${M_3}^2$ are similar to those of ${C_1}^2$.

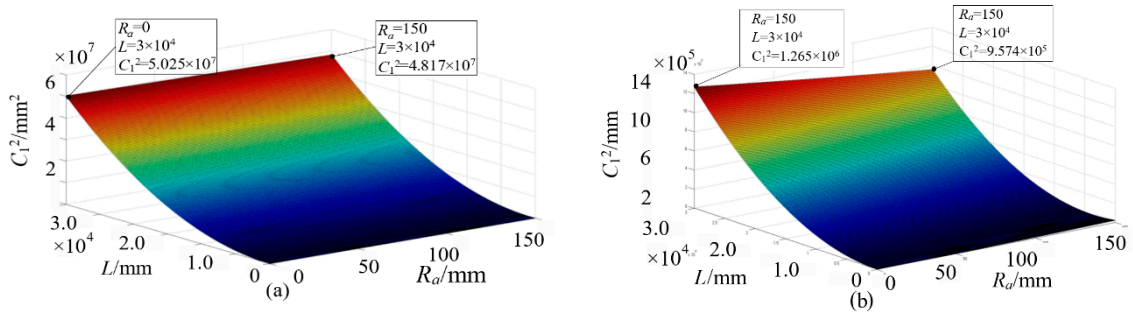

Figure 7. Change surface map of C_1. (**a**) corresponds to the same positive and negative α_r and γ_r, (**b**) corresponds to the difference between α_r and γ_r.

As shown in Equation (25), the coefficients C_2, N_2, and M_2 are affected by the parameter R_b. Since the values of α_b and β_b are usually small and N_2 is proportional to R_b, the value of C_2 can be decreased by decreasing the value of R_b.

$$\begin{cases} C_2 = \frac{\partial F_1 F_{2x}}{\partial \alpha_b} = R_b C\alpha_b C\Delta p + R_b S\alpha_b S\beta_b S\Delta p \\ N_2 = \frac{\partial F_y}{\partial \alpha_b} = R_b C\Delta p S\alpha_b S\beta_b - R_b C\alpha_b S\Delta p \\ M_2 = \frac{\partial F_z}{\partial \alpha_b} = R_b C\beta_b S\alpha_b \end{cases}, \tag{25}$$

$$\begin{cases} C_3 = \frac{\partial F_1 F_{2x}}{\partial \beta_b} = e_b S\beta_b S\Delta p - R_b C\alpha_b C\beta_b S\Delta p \\ N_4 = \frac{\partial F_y}{\partial \beta_b} = e_b S\beta_b C\Delta p - R_b C\alpha_b C\beta_b C\Delta p \\ M_4 = \frac{\partial F_z}{\partial \beta_b} = e_b C\beta_b + R_b C\alpha_b S\beta_b \end{cases}. \tag{26}$$

As shown in Equation (26), the coefficients C_3, N_4, M_4 are affected by the parameters e_b and R_b. The change surface of ${C_3}^2$ with e_b and R_b as variables is shown in Figure 8.

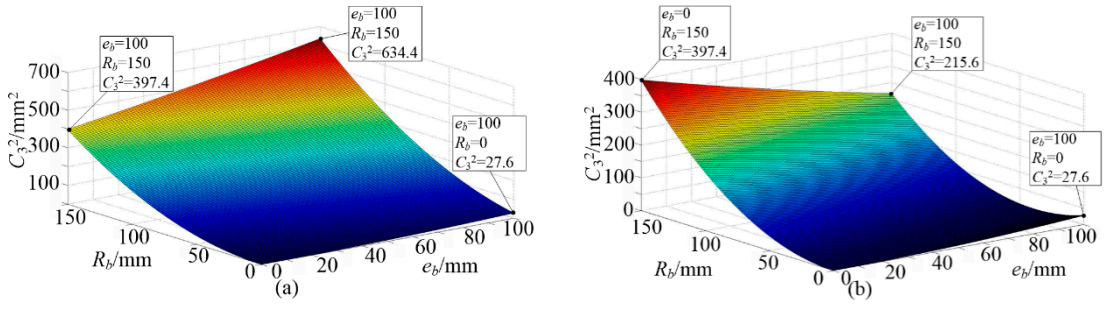

Figure 8. Change surface map of C_3. (**a**) corresponds to β_b less than 0, (**b**) corresponds to β_b greater than 0.

Figure 8a corresponds to β_b less than 0, and Figure 8b corresponds to β_b greater than 0. As can be seen from the figure, the parameter e_b has less influence on ${C_3}^2$, and ${C_3}^2$ is proportional to e_b. The maximum value is more than eight times the minimum value. The relative curves of ${N_4}^2$ and ${M_4}^2$ relative to parameters e_b and R_b are similar to those of ${C_3}^2$.

In summary, when the error transfer coefficient is related to the parameter L, it is mainly affected by the parameter L, and has little relationship with the parameters R_a and R_b. When the error transfer

coefficient is independent of L, its value is proportional to the parameters R_a and R_b and varies greatly. This can prove that the flange center based measuring device can reduce the error transfer coefficient of its mathematical model I by eliminating the parameters R_a and R_b.

4. Measurement Experiment of Measuring Device Based on Flange Center Positioning

4.1. Composition of the Measuring Device

The pipeline measuring experimental device based on the flange center positioning is composed of the measuring device I, the measuring device II, the winch, the pipeline, the PLC (Programmable Logic Controller) and the upper computer, as shown in Figure 9.

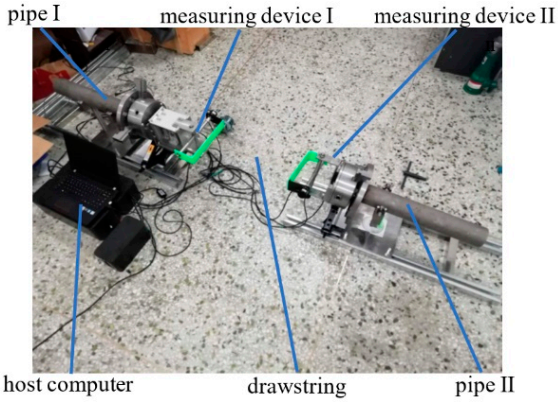

Figure 9. Measuring device based on flange center positioning.

Pipe I and pipe II are placed on the rails to move the pipe position. Pipe II can realize the horizontal and vertical swing adjustment and the vertical direction lift adjustment. During the experiment, different relative positional attitudes between the pipes can be simulated by moving pipe II and adjusting its horizontal, pitching, and vertical heights.

4.2. Testing Method and Recording Data

(1) First, the distance between the draw-out points of the two measuring devices from the end face of the pipe is measured. Then, adjust the height of pipe I to be equal to pipe II, and align the two rails of the installation pipe. Next, pipe II is moved to align the angle measuring mechanisms in the measuring device I and the measuring device II as shown in the Figure 10. At this time, the initial data of each sensor is collected by controlling the upper computer.

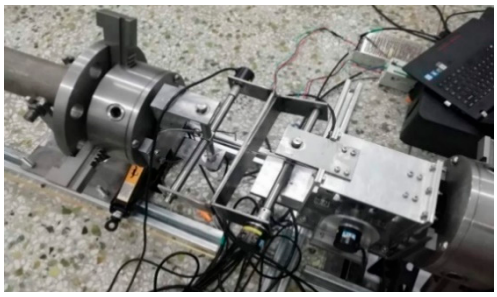

Figure 10. Initialization of measuring device based on flange center positioning.

(2) Move pipe II to a different position on the rail. The measurement data of each sensor is observed and recorded on the host computer, and the relative distance and angle of the two pipes are measured by the laser range finder and the angle measuring instrument as reference values.

(3) The measurement experiment based on the flange center positioning uses a laser rangefinder to adjust the distance between the two pipeline centers to 2 m, 3 m, 4 m, 5 m, 6 m, and 7 m, and the angle measuring instrument is used to adjust the angles parameters ξx_2, ξy_2, and ξz_2 formed by the axis of pipe II and the X, Y, and Z axes of the absolute coordinate system Ω_R. It corresponds to the actual value in Table 2. Then the host computer calculates the projection values $O_R O_{bx}$, $O_R O_{by}$, $O_R O_{bz}$, ξx_2, ξy_2, and ξz_2. It corresponds to the measurements in Table 2.

Table 2. Experimental data of measuring devices based on flange center positioning.

Component of Measurements	Classification	2 m	3 m	4 m	5 m	6 m	7 m
$O_r O_{bx}$	actual value (mm)	0.0	0.0	0.0	0.0	0.0	0.0
	measurements (mm)	4.7	9.2	13.1	16.8	23.1	30.5
$O_r O_{by}$	actual value (mm)	2000.0	3000.0	4000.0	5000.0	6000.0	7000.0
	measurements (mm)	1994.8	3004.1	4008.3	5014.8	6016.8	7025.2
$O_r O_{bz}$	actual value (mm)	0.0	0.0	0.0	0.0	0.0	0.0
	measurements (mm)	−2.1	9.6	11.9	18.8	32.5	46.9
ξx_2	actual value (mm)	0.0	0.0	0.0	0.0	0.0	0.0
	measurements (mm)	0.2	0.3	0.6	0.9	1.0	1.1
ξy_2	actual value (mm)	90.0	90.0	90.0	90.0	90.0	90.0
	measurements (mm)	89.8	89.5	89.3	89.0	89.1	88.9
ξz_2	actual value (mm)	0.0	0.0	0.0	0.0	0.0	0.0
	measurements (mm)	0.2	0.3	0.7	0.6	0.8	0.9

4.3. Analysis of Measurement Data

Comparing Tables 1 and 2, it is found that the experimental error of the measuring device based on the flange center positioning is smaller than that based on the outer circle positioning of the pipe, and the table shows the positioning method based on the flange center when the center distance between the two pipes is greater than 5 m and can reduce the error value of the measuring device by about 30%. In the 10 m working range, the error of Ox, Oy, and Oz was up to 56.49 mm, the precision was controlled within ±60 mm, and the system length measurement accuracy met the technical requirements. The maximum error of ξx, ξy and ξz was 0.588°, the accuracy was controlled within ±1°, and the system angle measurement accuracy met the technical requirements.

5. Conclusions

We have proposed a measuring device for measuring the pose of deep-sea pipelines. This measuring device measures the parameters used to calculate the pose of the pipeline using a drawstring pair. Moreover, we proposed a mathematical model of this device and solution formulas for calculating the pose of the pipeline. The measuring device we propose uses flanges for positioning on the pipe, which are smaller than the pin positioning error in the measuring device based on the outer circumference of the pipe. This measurement method is simpler than the measurement devices for underwater acoustic positioning and GPS positioning, and it is not easily interfered by the surrounding environment. At the same time, the structure and mathematical model of the proposed measuring device are simpler than those of the old tensioning rope measuring device.

In summary, the measurement device based on the flange center positioning has higher measurement accuracy, but the measurement device can be further improved. It can coincide the pull-out point of the measuring device based on the flange center positioning with the center point of the end face of the pipe. For example, the entire measuring device is transferred to the inside of the oil pipeline, and the mathematical model and solving formula of the measuring device will be simpler and more accurate. At this time, only the length of the drawstring and the data of the sensor need to be measured, and the spatial relative positions of the two pipes can be measured without knowing the two measurement parameters of e_a and e_b. Therefore, the error of the measuring device will be further reduced.

Author Contributions: The first author, Z.W., conceived the framework of the article and wrote the article; the second author, H.-x.D., analyzed the position and attitude measurement device based on the positioning of the outer wall of the submarine pipeline; the third author, T.W., designed and analyzed the measuring device based on the center positioning of submarine pipeline; the fourth author, B.Z., analyzes the experimental data of the measurement device based on the center positioning of the submarine pipeline. All authors have read and agreed to the published version of the manuscript.

Funding: This paper was funded by NSFC (Contract name: Research on ultimate bearing capacity and parametric design for the grouted clamps strengthening the partially damaged structure of jacket pipes). (Grant number: 51879063) and (Contract name: Research on analysis and experiments of gripping and bearing mechanism for large-scale holding and lifting tools on ocean foundation piles), (Grant number: 51479043).

Conflicts of Interest: The authors declare no conflict of interest.

References

1. Yu, X.C.; Wang, C.S.; Li, B.; Cheng, B.; Li, Y.; Wang, Q. Pigging Solutions Study of Subsea Tieback Flow line for Deep-water Oil and Gas Fields in the South China Sea. *Ocean Eng. Equip. Technol.* **2017**, *4*, 199–205.
2. Gao, Y.B.; Li, H.Q.; Chai, Y.P.; Ma, C.L. The Development of Deep Ocean High Technology. *Ocean Technol.* **2010**, *29*, 119–125.
3. De Lucena, R.R.; Baioco, J.S.; De Lima, B.S.L.P.; Albrecht, C.H.; Jacob, B.P. Optimal design of submarine pipeline routes by genetic algorithm with different constraint handling techniques. *Adv. Eng. Softw.* **2014**, *76*, 110–118. [CrossRef]
4. Laye, A.; Victoire, K.; Cocault-Duverger, V. Model-Centric Digital Subsea Pipeline Design Process and Framework. In Proceedings of the Offshore Technology Conference, Houston, TX, USA, 30 April–3 May 2018.
5. Wang, L.Q.; Pan, Z.J.; Zhao, D.Y.; He, N.; Zhang, L. Technology of Pipeline Alignment in Subsea. *Mach. Tool Hydraul.* **2010**, *38*, 16–27.
6. Wang, D.Y.; Zhu, A.D. Current Situation of Offshore Petroleum Equipment and Development Orientation of Localization. *Chin. Pet. Mach.* **2014**, *42*, 33–39.
7. Liu, F. Method Study for Subsea Pipeline Spool Installation and Design in Special Working Condition. *Pipeline Technol. Equip.* **2018**, *151*, 34–41.
8. Zhao, J.H.; Ouyang, Y.Z.; Wang, A.X. Status and Development Tendency for Seafloor Terrain Measurement Technology. *Acta Geod. Cartogr. Sin.* **2017**, *46*, 1786–1792.
9. Dariusz, P.; Tomasz, T.; Michał, L. Using the geodetic and hydroacoustic measurements to investigate the bathymetric and morphometric parameters of Lake Hańcza. *Open Geosci.* **2015**, *7*, 1–8.
10. Getmanov, V.G.; Modyaev, A.D.; Firsov, A.A. A method of measurement of the coordinates of a moving object with the use of a passive hydroacoustic detection and ranging system. *Meas. Technol.* **2012**, *55*, 248–256. [CrossRef]
11. Tomasz, P. Correction of Navigational Information Supplied to Biomimetic Autonomous Underwater Vehicle. *Pol. Marit. Res.* **2018**, *25*, 13–22.
12. Gamroth, E.; Kennedy, J.; Bradley, C. Design and testing of an acoustic ranging technique applicable for an underwater positioning system. *Underwater Technol.* **2011**, *29*, 4467–4477. [CrossRef]
13. Wang, L.Q.; Wang, W.M.; Zhao, D.Y.; Cao, W.; Wang, C.D. A research into the Flange Connection Tooling for deep-sea pipelines. *Nat. Gas Ind.* **2009**, *29*, 89–97.
14. Zhu, S.H.; Wei, X.C.; Liu, B. Study and application of measure technology by flange measure instrument to spool piece connection of subsea pipelines. *Chin. Offshore Oil Gas* **2008**, *20*, 342–349.
15. Den, N.S.; Oljeselskap, A.S. System for subsea diverless metrology and hard-pipe connection of pipelines. U.S. Patent 6700835, 2 March 2004.
16. Wang, W.M.; Wang, C.D.; Wang, L.Q. A novel deepwater structures pose measurement method and experimental study. *Measurement* **2012**, *45*, 1151–1159. [CrossRef]
17. Shabani, M.; Gholami, A. Improved Underwater Integrated Navigation System using Unscented Filtering Approach. *J. Navig.* **2016**, *69*, 561–570. [CrossRef]

18. Mallios, A.; Vidal, E.; Campos, R.; Carreras, M. Underwater caves sonar data set. *Int. J. Rob. Res.* **2017**, *36*, 1247–1256. [CrossRef]
19. Han, W.H.; Zhou, J. Comparative Research of Corrosion Models for Corroded Submarine Pipelines. *Pet. Eng. Constr.* **2014**, *40*, 9–17.